# Based on Robust Sliding Mode and Linear Active Disturbance Rejection Control for Attitude of Quadrotor Load UAV

**Zhaoji Wang** ( 1657805643@qq.com )
Qingdao University of Science and Technology
**Tong Zhao**
Qingdao University of Science and Technology

**Research Article**

**Keywords:** Quadrotor, Attitude Control, Sliding Mode Control, Mass Variation, Adaptive Control, Linear Active Disturbance Rejection Control

**Posted Date:** August 2nd, 2021

**DOI:** https://doi.org/10.21203/rs.3.rs-735025/v1



**Version of Record:** A version of this preprint was published at Nonlinear Dynamics on March 19th, 2022.
See the published version at https://doi.org/10.1007/s11071-022-07349-y.

# Based on robust sliding mode and linear active disturbance rejection control for attitude of quadrotor load UAV

Author Name: Zhaoji Wang

Affiliation: School of Automation & Electronic Engineering, Qingdao University of Science and Technology, 266061 China

Author(s) Emails: 1657805643@qq.com

Corresponding Author Name: Tong Zhao

Position: Dr. / Prof.

Affiliation: School of Automation & Electronic Engineering, Qingdao University of Science and Technology, 266061 China

Author(s) Emails: zt66516@163.com

**Abstract:** In this paper, a mass adaptive control method combining robust sliding mode control (SMC) and linear active disturbance rejection control (LADRC) is designed for the quadrotor load unmanned aerial vehicle (UAV) with mass variation. The scheme combines the advantages of SMC and LADRC. SMC can enhance the robustness of the controller, improve the anti-disturbance performance and overcome the problem of low control precision caused by bandwidth limitation of LADRC. The linear extended state observer (LESO) can estimate the external and internal disturbances of the system in real time, and then compensate the total disturbance through the PD controller. In order

to simplify parameter setting, adaptive control is introduced in LADRC to adjust controller parameters in real time. In addition, adaptive law is also used to control the mass variation of the quadrotor. Then the stability of the whole system is verified by Lyapunov stability theory. Finally, the comparison with LADRC shows the superiority of the designed scheme, which can track the reference signal stably and effectively.

**Keywords:** Quadrotor, Attitude Control, Sliding Mode Control, Mass Variation, Adaptive Control, Linear Active Disturbance Rejection Control

## 1.Introduction

The quadrotor UAV has the advantages of simple structure and strong maneuverability. It has become a research hotspot and has been widely used in many fields [1,2]. The quadrotor load UAV can carry out tasks such as object handling, rescue and data collection [3], so the research on the quadrotor cannot be ignored.

The quadrotor has a complicated mathematical model, which makes it particularly difficult to design its control scheme. In [4], a robust PID controller is proposed to realize the quadrotor trajectory tracking task. Considering the rotation and translation of the quadrotor, a nonlinear PID algorithm is designed in [5]. Aiming at the yaw and altitude channels of the quadrotor, a multiple-model adaptive controller is designed in [6]. Aiming at the model uncertainty and unknown disturbance of the quadrotor, a robust adaptive recursive sliding mode control scheme is adopted in [7]. In [8], considering the attitude and altitude control of the quadrotor system with bounded disturbances, an adaptive non-singular terminal SMC is proposed. Taking into account

the disturbances of the quadrotor during the trajectory tracking, a global SMC algorithm is proposed in [9]. In [10], in order to ensure that the quadrotor can effectively track the desired trajectory, a multilayer neural dynamic controller is designed.

The active disturbance rejection control (ADRC) technology is simple structure and strong control performance, and it does not need the accurate mathematical model, so it can be used in quadrotor system with nonlinear and strong coupling [11]. In [12], the obstacle avoidance function of the quadrotor is realized by the ADRC. In [13], the ADRC technology is adopted to enhance the anti-disturbance performance of the quadrotor system. In [14], ADRC is used to solve the input delay and external disturbances of the quadrotor. In view of the complex coupling and strong nonlinearity of the powered parafoil system, an ADRC scheme is used in [15] to compensate its coupling. In the airship system, an ADRC scheme is adopted to control its horizontal trajectory tracking [16]. However, the traditional ADRC contains nonlinear functions and many parameters, which makes parameter tuning complicated. Therefore, Gao introduces the concept of bandwidth and proposes a linear active disturbance rejection controller (LADRC) with fewer parameters, which consists of a PD controller and a linear extended state observer (LESO) [17]. The LADRC retains the advantages of strong anti-disturbance ability and simple structure, and also reduces the adjustable parameters, which greatly improves its application in actual engineering. Aiming at the strong coupling and nonlinearity of the quadrotor system, an improved LADRC strategy is proposed in [18]. In [19], the LADRC is adopted to estimate and compensate the disturbances of variable speed micro-hydro plant in real time. In order to solve the

oscillatory system with time delay, LADRC is adopted to compensate the time delay in [20]. In [21], a LADRC control scheme is proposed to control the steam temperature of boiler outlet. Despite the above advantages, LADRC has strong correlation among its parameters, which leads to the complexity of parameter tuning. Moreover, it is well known that although a higher bandwidth can better track the expected signal and suppress disturbance, the bandwidth in the practical application is limited by the dynamic uncertainties. In addition, high bandwidth may cause oscillations and even lead to system instability, as well as increase operating costs. Therefore, in practical applications, bandwidth is limited by the requirements of performance and dynamic uncertainty, which leads to a decrease in the control precision of LADRC.

In the existing research on the quadrotor, most of them are established the mathematical model of the quadrotor by assuming that its mass is constant. However, this assumption may not hold true in practical application. For example, the quadrotor is used for carrying objects, pesticide spraying, etc. Its mass is variable, which will lead to the position of its centroid to change and cause time-varying disturbances, thus affecting its control precision. Therefore, the time-varying mass problem should be considered in the process of quadrotor modeling.

In this paper, we have established a more accurate mathematical model and proposed a control scheme that combines robust SMC and LADRC. The main contributions of this paper are as follows:

(1) The mathematical model of the quadrotor load UAV is established, which takes into account the air resistance, the position of centroid and the moments acting on the

quadrotor to make the established model more accurate. In addition, the adaptive law is introduced for the problem of mass variation.

(2) A control scheme combining robust SMC and LADRC is proposed. The scheme combines the advantages of both. LESO is used to estimate the internal and external disturbances of the system and compensate it with the PD controller. SMC can further enhance the robustness of the controller and overcome the shortcomings of low control precision of LADRC due to limited bandwidth.

(3) In view of the strong correlation of LADRC parameters, the introduction of adaptive control can adjust the parameters of controller in real time according to the state of the system, which greatly simplifies the parameter setting process, and also provides a novel method for proving the stability of the whole controller.

(4) The system is verified to be stable by using Lyapunov stability theory, the simulation results are compared with LADRC to verify that the designed scheme has strong anti-disturbance ability and fast response speed, which proves its effectiveness.

The rest of this article is structured as follows: The mathematical model of the quadrotor is established in Section 2; The control scheme is given in section 3; Section 4, the stability analysis of the system is given; Section 5 is the simulation results and discussion; Section 6 summarizes the paper.

## 2. Mathematical model

According to Figure 1, the quadrotor can be modelled using six coordinates, namely $x$ , $y$ and $z$ for the position coordinates, and $\phi$ , $\theta$ and $\psi$ for the attitude

coordinates [22]. When the quadrotor is loaded, its center of mass moves down from the origin of the body fixed frame $B$. The dynamics model of the quadrotor load UAV is established with reference to the earth fixed frame $E$ and the body fixed frame $B$ [23].

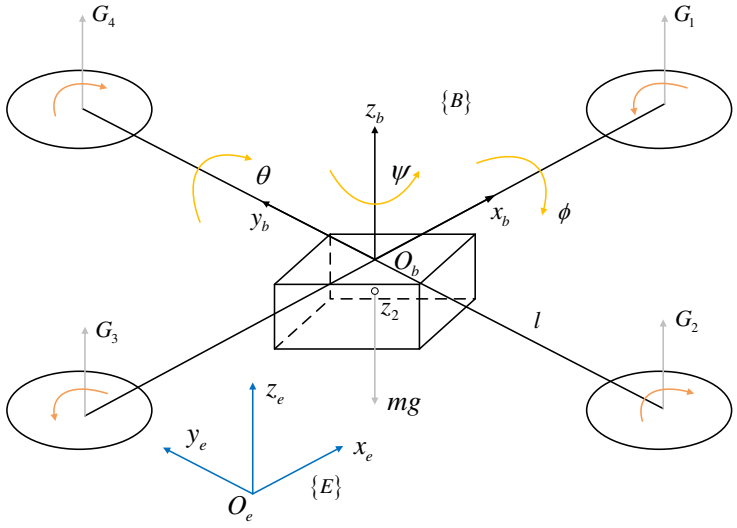


Fig.1 Structure diagram of a quadrotor load UAV

According to the matrix transformation relationship between the earth fixed frame $E$ and the body fixed frame $B$ [24, 25], the following formula can be obtained

$$\begin{aligned} R&=R(z,\psi)R(y,\theta)R(x,\phi) \\ &=\begin{bmatrix} \cos\psi & -\sin\psi & 0 \\ \sin\psi & \cos\psi & 0 \\ 0 & 0 & 1 \end{bmatrix}\begin{bmatrix} \cos\theta & 0 & \sin\theta \\ 0 & 1 & 0 \\ -\sin\theta & 0 & \cos\theta \end{bmatrix}\begin{bmatrix} 1 & 0 & 0 \\ 0 & \cos\phi & -\sin\phi \\ 0 & \sin\phi & \cos\phi \end{bmatrix} \\ &=\begin{bmatrix} \cos\theta\cos\psi & \sin\theta\sin\phi\cos\psi-\cos\phi\sin\psi & \sin\theta\cos\psi\cos\phi+\sin\phi\sin\psi \\ \cos\theta\sin\psi & \sin\theta\sin\phi\sin\psi+\cos\phi\cos\psi & \sin\theta\sin\psi\cos\phi-\sin\phi\cos\psi \\ -\sin\theta & \cos\theta\sin\phi & \cos\theta\cos\phi \end{bmatrix} \end{aligned} \tag{1}$$

With the consideration of Newton's second law, the position dynamics model of the quadrotor load UAV is obtained as

$$\begin{cases} \dot{V}_E = V \\ M\dot{V} + m\dot{V} = G_E + Mg + mg + K_{f1} \end{cases} \tag{2}$$

where $V_E = [x \quad y \quad z]^T$; $V$ is the linear velocity of the quadrotor in the earth fixed

frame $E$; $G_E$ is the total lift provided by the four motors; $M$ is the mass of the quadrotor; $m$ is the mass of the load; $g$ is the acceleration due to gravity; $K_{f1} = [-k_f \dot{x} \quad -k_f \dot{y} \quad -k_f \dot{z}]^T$ is the air resistance matrix, $k_f$ is the air resistance coefficient.

Considering the body fixed frame $B$, the total lift of UAV is as follows

$$G_B = [G_x \quad G_y \quad G_z]^T = [0 \quad 0 \quad G]^T \tag{3}$$

where $G = \sum_{i=1}^{4} G_i = G_1 + G_2 + G_3 + G_4$, according to the transformation formula between the earth fixed frame $E$ and the body fixed frame $B$, it can obtain

$$G_E = RG_B = R\begin{bmatrix} 0 \\ 0 \\ G \end{bmatrix} = G\begin{bmatrix} \sin\theta\cos\psi\cos\phi + \sin\phi\sin\psi \\ \sin\theta\sin\psi\cos\phi - \sin\phi\cos\psi \\ \cos\theta\cos\phi \end{bmatrix} \tag{4}$$

According to formulas (2) and (4), the position dynamics model of the quadrotor load UAV is as follows

$$\begin{cases} \ddot{x} = G(\sin\theta\cos\psi\cos\phi + \sin\phi\sin\psi)/(M+m) - k_f\dot{x}/(M+m) \\ \ddot{y} = G(\sin\theta\sin\psi\cos\phi - \sin\phi\cos\psi)/(M+m) - k_f\dot{y}/(M+m) \\ \ddot{z} = G\cos\theta\cos\phi/(M+m) - g - k_f\dot{z}/(M+m) \end{cases} \tag{5}$$

When the quadrotor UAV is loaded, its center of mass shifts downward, resulting in an increase in the distance from the motor to the centroid, which affects the pitch and roll angle movement of the quadrotor. The quadrotor carries the load through the mount platform, and the two can be regarded as a whole. The centroid coordinate of the quadrotor is $(x_1, y_1, z_1)$, the centroid coordinate of the load is $(x_2, y_2, z_2)$. The following formula gives the mathematical method of determining the position of the centroid.

$$\begin{cases} x_a = (x_1 M + x_2 m)/(M+m) \\ y_a = (y_1 M + y_2 m)/(M+m) \\ z_a = (z_1 M + z_2 m)/(M+m) \end{cases} \tag{6}$$

where $(x_a, y_a, z_a)$ is the centroid coordinate of the quadrotor load UAV. According to Fig.1, the centroid coordinates of the quadrotor and the load are $(0,0,0)$ and $(0,0,z_2)$ respectively. Substituting into the above equation, the centroid coordinates of the quadrotor load UAV can be obtained as $(0,0,z_a)$.

$$z_a = z_2 m/(M+m) \tag{7}$$

Considering the Newton-Euler equation [26, 27], the attitude dynamics model is written as

$$\begin{cases} I\dot{\Omega} + \Omega \times I\Omega = M \\ M = N + O + K_{f2} \end{cases} \tag{8}$$

where $I = diag(I_x, I_y, I_z)$ is the moment of inertia matrix; $\Omega = [\dot{\phi} \ \dot{\theta} \ \dot{\psi}]^T$ is the angular velocity of the quadrotor rotating about each axis; $M$ is the resultant moment acting on the quadrotor; $K_{f2} = [-lk_f\dot{\phi} \ -lk_f\dot{\theta} \ -k_f\dot{\psi}]^T$ is the resistance moment; $N$ and $O$ are the pulling moment and reaction torque of the quadrotor, respectively.

$$N = \begin{bmatrix} b_1\sqrt{l^2+z_a^2}(-G_1+G_2+G_3-G_4) \\ b_1\sqrt{l^2+z_a^2}(-G_1-G_2+G_3+G_4) \\ 0 \end{bmatrix} \tag{9}$$

$$O = \begin{bmatrix} 0 \\ 0 \\ b_2(G_1-G_2+G_3-G_4) \end{bmatrix} \tag{10}$$

where $b_1$ is the lift coefficient; $b_2$ is the anti-torque coefficient; $l$ is the length of the quadrotor arm.

According to formulas (8) (9) and (10), the attitude dynamics of the quadrotor is

obtained as

$$\begin{cases} \ddot{\phi} = b_1\sqrt{l^2+z_a^2}(-G_1+G_2+G_3-G_4)/I_x + (I_y-I_z)\dot{\theta}\dot{\psi}/I_x - lk_f\dot{\phi}/I_x \\ \ddot{\theta} = b_1\sqrt{l^2+z_a^2}(-G_1-G_2+G_3+G_4)/I_y + (I_z-I_x)\dot{\phi}\dot{\psi}/I_y - lk_f\dot{\theta}/I_y \\ \ddot{\psi} = b_2(G_1-G_2+G_3-G_4)/I_z + (I_x-I_y)\dot{\phi}\dot{\theta}/I_z - k_f\dot{\psi}/I_z \end{cases} \tag{11}$$

where $\phi$, $\theta$ and $\psi$ are respectively the roll, pitch and yaw angles of the quadrotor UAV.

Use the virtual control variables $(U_1, U_2, U_3, U_4)$ to simplify the dynamic model, as shown in the following formula

$$\begin{bmatrix} U_1 \\ U_2 \\ U_3 \\ U_4 \end{bmatrix} = \begin{bmatrix} \frac{1}{(M+m)} & \frac{1}{(M+m)} & \frac{1}{(M+m)} & \frac{1}{(M+m)} \\ -\frac{b_1}{I_x} & \frac{b_1}{I_x} & \frac{b_1}{I_x} & -\frac{b_1}{I_x} \\ -\frac{b_1}{I_y} & -\frac{b_1}{I_y} & \frac{b_1}{I_y} & \frac{b_1}{I_y} \\ \frac{b_2}{I_z} & -\frac{b_2}{I_z} & \frac{b_2}{I_z} & -\frac{b_2}{I_z} \end{bmatrix} \begin{bmatrix} G_1 \\ G_2 \\ G_3 \\ G_4 \end{bmatrix} \tag{12}$$

According to the above formula, the dynamic model of the quadrotor load UAV is written in the following form

$$\begin{cases} \ddot{x} = U_1(\sin\theta\cos\psi\cos\phi + \sin\phi\sin\psi) - k_f\dot{x}/(M+m) \\ \ddot{y} = U_1(\sin\theta\sin\psi\cos\phi - \sin\phi\cos\psi) - k_f\dot{y}/(M+m) \\ \ddot{z} = U_1\cos\theta\cos\phi - g - k_f\dot{z}/(M+m) \\ \ddot{\phi} = U_2\sqrt{l^2+z_a^2} + (I_y-I_z)\dot{\theta}\dot{\psi}/I_x - lk_f\dot{\phi}/I_x \\ \ddot{\theta} = U_3\sqrt{l^2+z_a^2} + (I_z-I_x)\dot{\phi}\dot{\psi}/I_y - lk_f\dot{\theta}/I_y \\ \ddot{\psi} = U_4 + (I_x-I_y)\dot{\phi}\dot{\theta}/I_z - k_f\dot{\psi}/I_z \end{cases} \tag{13}$$

The quadrotor dynamics model in formula (13) can also be expressed in the following form [28].

$$\begin{cases} \dot{u}_1 = u_2 \\ \dot{u}_2 = Qv(n) + P + b \end{cases} \tag{14}$$

where $u_1 = [z \quad \phi \quad \theta \quad \psi]^T$ , $u_2 = [\dot{z} \quad \dot{\phi} \quad \dot{\theta} \quad \dot{\psi}]^T$ , $v(n) = [U_1 \quad U_2 \quad U_3 \quad U_4]^T$ ,

$$Q = \begin{bmatrix} \cos\theta\cos\phi & 0 & 0 & 0 \\ 0 & \sqrt{l^2 + z_a^2} & 0 & 0 \\ 0 & 0 & \sqrt{l^2 + z_a^2} & 0 \\ 0 & 0 & 0 & 1 \end{bmatrix}, \quad P = \begin{bmatrix} -g - k_f \dot{z}/(M+m) \\ (I_y - I_z)\dot{\theta}\dot{\psi}/I_x - lk_f\dot{\phi}/I_x \\ (I_z - I_x)\dot{\phi}\dot{\psi}/I_y - lk_f\dot{\theta}/I_y \\ (I_x - I_y)\dot{\phi}\dot{\theta}/I_z - k_f\dot{\psi}/I_z \end{bmatrix}.$$

## 3. Control scheme design

Aiming at the problems of strong coupling, nonlinear and mass variation of the quadrotor load UAV, this section proposes a control scheme combining robust sliding mode control and LADRC, and establishes an adaptive control of mass. The following Fig.2 shows the block diagram of the control scheme.

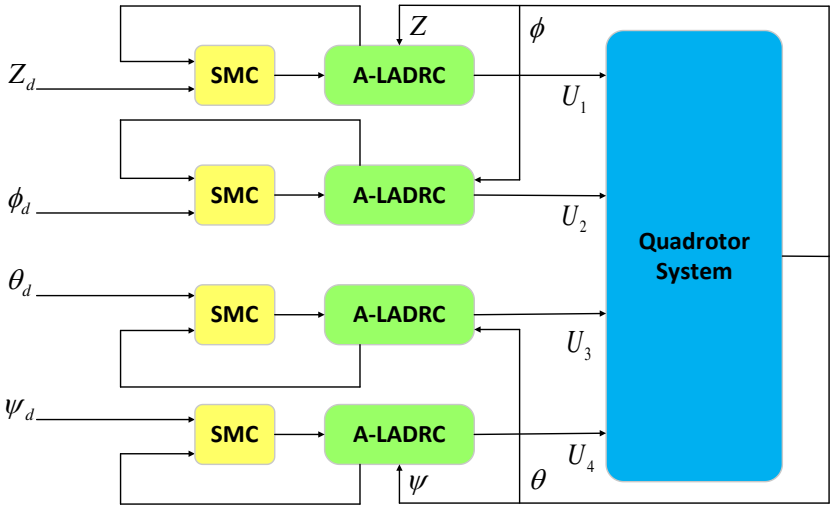


Fig.2 Block diagram of control scheme

The attitude channel and altitude channel of the quadrotor are controlled by SMC and LADRC, which can effectively reduce the influence of external disturbances on the quadrotor, and LADRC can also eliminate the coupling between each channel and improve the performance of the overall control scheme. In addition, in order to simplify the parameter setting and eliminate the problem of time-varying mass, adaptive control

is adopted to adjust the parameters and mass variation in real time.

3.1 Design of linear active disturbance rejection control

The quadrotor is subject to various disturbances in flight, The LADRC can effectively eliminate the influence of disturbances on the quadrotor and improve the anti-disturbance performance of the controller [29]. Fig.3 shows the structure diagram of the controller.

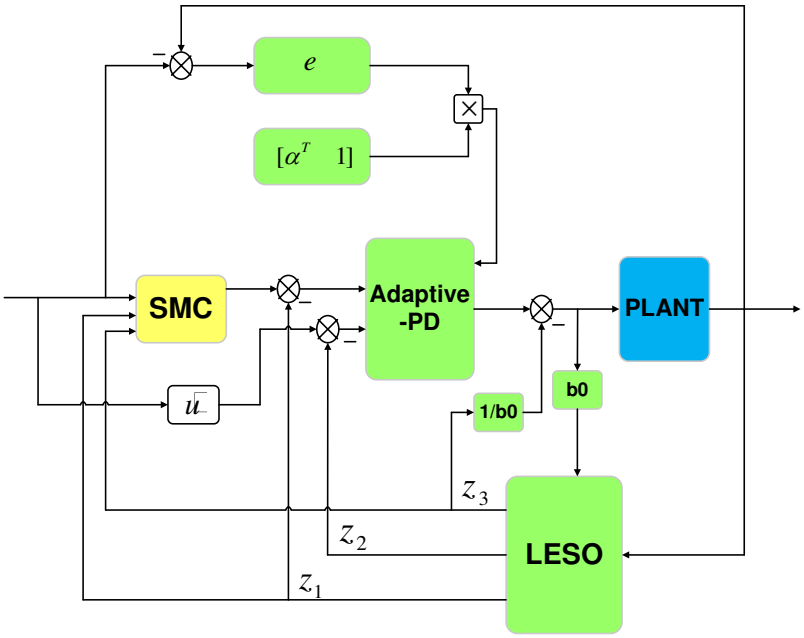


Fig.3 Structure diagram of controller

The dynamics of the quadrotor in formula (14) is written into the nonlinear system in the following form.

$$\begin{cases} \dot{u}_1 = u_2 \\ \dot{u}_2 = Qv(n) + P + b \\ y = u_1 \end{cases} \tag{15}$$

where $u = \begin{bmatrix} u_1 & u_2 \end{bmatrix}^T$ is the measurable system state; $Q$ and $P$ are the nonlinear functions of the system; $b$ is the external disturbances.

The total disturbance of the system is designed in the following form

$$H(u, v(n)) = P + Qv(n) + b \tag{16}$$

In order to estimate the total disturbance, $z_1 = u$, $z_2 = \dot{u}$ and $z_3 = H(u, v(n))$ are defined as extended state space representations of the system, where $z = [z_1 \quad z_2 \quad z_3]^T$.

The nonlinear system (15) can be obtained as

$$\begin{cases} \dot{z} = Az + Bv + Ch \\ y = Dz \end{cases} \tag{17}$$

where $A = \begin{bmatrix} 0 & 1 & 0 \\ 0 & 0 & 1 \\ 0 & 0 & 0 \end{bmatrix}$, $B = [0 \quad b_0 \quad 0]^T$, $C = [0 \quad 0 \quad 1]^T$, $D = [1 \quad 0 \quad 0]$, $h = \dot{H}(u, v)$.

$z$ can be obtained in real time through the LESO.

$$\begin{cases} \dot{\hat{z}} = A\hat{z} + Bv + \eta(y - \hat{y}) \\ \hat{y} = D\hat{z} \end{cases} \tag{18}$$

where $\eta = [\eta_1 \quad \eta_2 \quad \eta_3]^T$ is the gain vector of LESO.

**Remark 1:** The LESO can treat the combined effect of the unknown external and internal disturbances of the system as extended state, and observe this extended state through output feedback, then use the PD controller to compensate. In addition, the LESO does not depend on the specific mathematical model of the system, it is only related to the order of the plant.

The gain of the observer is parameterized by the characteristic equation, it can be obtained that

$$\Upsilon(s) = s^3 + \eta_1 s^2 + \eta_2 s + \eta_3 = (s + \omega)^3 \tag{19}$$

where $\eta = \left[3\omega \quad 3\omega^2 \quad \omega^3\right]^T$, $\omega$ is the bandwidth of LESO.

**Remark 2:** The increase of the bandwidth $\omega$ of LESO is helpful to improve the

control precision of LADRC, but increasing $\omega$ will cause the output of the controller to increase, which is not conducive to the practical application of engineering. In addition, the high bandwidth will also cause oscillation and lead to system instability. Therefore, in practical applications, the control precision of LADRC is reduced due to the limitation of bandwidth. In order to solve this problem, this paper introduces SMC to improve the overall performance of the controller.

It is defined that the estimated values of the extended state space representation of the system are $\hat{z}_1 = \hat{u}$, $\hat{z}_2 = \dot{\hat{u}}$ and $\hat{z}_3 = \hat{H}(u, v(n))$. The control law is designed as

$$u_l = (u_p - \hat{z}_3) / b_0 \tag{20}$$

where $u_p$ is the output of PD controller.

$$u_p = k_p(U_s - \hat{z}_1) + k_d(\dot{u}_d - \hat{z}_2) + \ddot{u}_d \tag{21}$$

**Remark 3:** In order to simplify the parameter setting, adaptive control is introduced to adjust $k_p$ and $k_d$ in real time, which is beneficial to the stability analysis of the whole quadrotor system and provides a novel method to enhance the stability of the controller. Formulas (36) and (37) give the adaptive law of $k_p$ and $k_d$, and the adaptive adjustment curves of $k_p$ and $k_d$ are given in Fig.7.

3.2 Design of sliding mode controller

The SMC has the characteristics of easy implementation and strong robustness [30]. The introduction of SMC can further improve the anti-disturbance performance of the controller and solve the problem of lower control precision of LADRC.

The sliding surface can be designed as

$$s = w_1 e_1 + \dot{e}_1 \tag{22}$$

where $w_1$ is the adjustable parameter, $e_1 = z_1 - u_d$ is the tracking error, $z_1$ is the estimation of the system state $u$ by the LESO, $u_d$ is the input signal of the system.

$$\begin{aligned} \dot{s} &= w_1 \dot{e}_1 + \ddot{e}_1 \\ &= w_1 \dot{e}_1 + \ddot{z}_1 - \ddot{u}_d \\ &= w_1 \dot{e}_1 + z_3 + b_0 v - \ddot{u}_d \end{aligned} \tag{23}$$

where $z_3$ is LESO's estimate of the total disturbance.

With the consideration of (23), the sliding mode control law is designed in the following form

$$U_s = \ddot{u}_d - w_1 \dot{e}_1 - z_3 - w_2 s \tag{24}$$

where $w_2$ is a positive parameter.

**Remark 4:** In order to ensure that the designed sliding mode control is stable and effective, an appropriate parameter $w_2$ is selected to satisfy $w_2 > 0$, which is proved by formula (46).

3.3 Adaptive law design for parameters adjustment

According to the tracking error $e_2 = u - u_d$, the filter tracking error is obtained as

$$\delta = \begin{bmatrix} \alpha^T & 1 \end{bmatrix} e_2 \tag{25}$$

where $\alpha = t_1$ is the appropriately chosen coefficient, so that when $\delta \to 0$, it satisfies $e_2 \to 0$.

Take the derivative of $\delta$ to get

$$\dot{\delta} = \dot{u}_2 - \ddot{u}_d + \begin{bmatrix} 0 & \alpha^T \end{bmatrix} e_2 \tag{26}$$

where

$$\dot{u}_2 = Qv(n) + P + b = H(u, v(n)) \tag{27}$$

The feedback linearization method is used to define the tracking control of the input signal to achieve the approximate purpose. As shown in the following formula

$$n = \hat{H}^{-1}(u, \gamma) \tag{28}$$

where $\gamma = \hat{H}(u,n)$ is pseudo control [31, 32], $\hat{H}(u,n)$ is any approximation of $H(u,v)$.

By adding and subtracting $\hat{H}(u,n)$ to the right of formula (27), we can get

$$\dot{u}_2 = \tilde{H}(u,v,n) + \hat{H}(u,n) \tag{29}$$

Assumption 2: $\hat{H}(u,n)$ is an arbitrary approximation of $H(u,v)$, so $\tilde{H}(u,v,n)$ is close to zero.

The pseudo control design is as follows

$$\gamma = -a\delta + u_p - \begin{bmatrix} 0 & \alpha^T \end{bmatrix} e_2 \tag{30}$$

where $a$ is any positive parameter.

Substituting formulas (21), (29) and (30) into (26), the derivative of the filtering tracking error is obtained as

$$\dot{\delta} = -a\delta + k_p(U_s - \hat{z}_1) + k_d(\dot{u}_d - \hat{z}_2) \tag{31}$$

3.4 Adaptive law design for mass variation

In this article, we mainly study the attitude control of the quadrotor load UAV, so the adaptive law of mass is established according to the altitude channel. It can be obtained from formulas (15) and (26).

$$\dot{\delta}_z = U_1 \cos\theta\cos\phi - g - k_f \dot{z}/(M+m) - \ddot{z}_d + \begin{bmatrix} 0 & \alpha^T \end{bmatrix} e_2 \tag{32}$$

According to the certainty equivalence principle can be obtained

$$U_1 = [-r\delta_z - \begin{bmatrix} 0 & \alpha^T \end{bmatrix} e_2 + \ddot{x}_d + g + k_f \dot{x}_d (M + \hat{m})] / (\cos\theta \cos\phi) \tag{33}$$

where $r > 0$ is an adjustable parameter, $\hat{m}$ is an estimate of the mass of the load. Substituting formula (33) into formula (32) can obtain

$$\dot{\delta}_z = -r\delta_z + k_f \dot{x}_d (M + \hat{m}) - k_f \dot{x}_d (M + m) \tag{34}$$

Let $\hat{M}_c = 1/(M + \hat{m})$, $M_c = 1/(M + m)$, The above formula is rewritten as follows

$$\dot{\delta}_z = -r\delta_z + k_f \dot{x}_d \hat{M}_c - k_f \dot{x}_d M_c \tag{35}$$

**4. Stability analysis**

**Theorem 1:** Consider the nonlinear system in formula (15), the following adaptive law is applied to make the assumption valid.

$$\dot{\hat{k}}_p = [\delta k_p (U_s - \hat{z}_1) \vartheta] / \tilde{k}_p \tag{36}$$

$$\dot{\hat{k}}_d = [\delta k_d (\dot{u}_d - \hat{z}_2) \zeta] / \tilde{k}_d \tag{37}$$

$$\dot{\hat{M}}_c = \varepsilon \delta_z k_f \dot{x}_d \tag{38}$$

where $\vartheta$, $\zeta$ and $\varepsilon$ are the appropriately selected parameters.

**Remark 5:** In order to eliminate the singularity problem that may exist in the adaptive law (36) and (37) when $\tilde{k}_p$ and $\tilde{k}_d$ are zero. Integrating $\dot{\hat{k}}_p$ and $\dot{\hat{k}}_d$ can write the adaptive law in the following form

$$\hat{k}_p = \int_0^t [\delta k_p (U_s - \hat{z}_1) \vartheta] / \tilde{k}_p d\tau + k_{p0} \tag{39}$$

$$\hat{k}_d = \int_0^t [\delta k_d (\dot{u}_d - \hat{z}_2) \zeta] / \tilde{k}_d d\tau + k_{d0} \tag{40}$$

where $\hat{k}_p$ and $\hat{k}_d$ are the estimated values of the controller parameters. As long as the appropriate constants $k_{p0}$ and $k_{d0}$ are selected, it can be ensured that $\tilde{k}_p = k_p - \hat{k}_p$ and $\tilde{k}_d = k_d - \hat{k}_d$ are not zero.

**Assumption 3:** The signals of the whole system are bounded and the tracking error converges to the neighborhood of zero.

**Proof of Theorem 1:** The positive definite Lyapunov function of the following form is designed

$$V=\frac{1}{2}s^2+\frac{1}{2}\delta^2+\frac{1}{2}\delta_z^2+\frac{1}{2}k_p^{T}\vartheta^{-1}k_p+\frac{1}{2}k_d^{T}\zeta^{-1}k_d+\frac{1}{2}M_c^{T}\varepsilon^{-1}M_c \tag{41}$$

Take the derivative of the above formula

$$\dot{V}=s\dot{s}+\delta\dot{\delta}+\delta_z\dot{\delta}_z+k_p^{T}\vartheta^{-1}\dot{k}_p+k_d^{T}\zeta^{-1}\dot{k}_d+M_c^{T}\varepsilon^{-1}\dot{M}_c \tag{42}$$

Substituting formulas (22), (31) and (35) into the above formula can obtain

$$\begin{aligned}\dot{V}&=s(w_1\dot{e}_1+\ddot{x}_d)+\delta[-a\delta+k_p(U_s-\hat{z}_1)+k_d(\dot{u}_d-\hat{z}_2)]+\delta_z(-r\delta_z+k_f\hat{M}_c-k_f\dot{M}_c)\\&\quad+k_p^{T}\vartheta^{-1}\dot{k}_p+k_d^{T}\zeta^{-1}\dot{k}_d+M_c^{T}\varepsilon^{-1}\dot{M}_c\\&=s(w_1\dot{e}_1+\ddot{x}_d-\dot{u}_d)-a\delta^2+\delta k_p(U_s-\hat{z}_1)+\delta k_d(\dot{u}_d-\hat{z}_2)-r\delta_z^2+\delta_z k_f\hat{M}_c\\&\quad+k_p^{T}\vartheta^{-1}\dot{k}_p+k_d^{T}\zeta^{-1}\dot{k}_d+M_c^{T}\varepsilon^{-1}\dot{M}_c\\&=s(w_1\dot{e}_1+z_3+U_s-\dot{u}_d)-a\delta^2+\delta k_p(U_s-\hat{z}_1)+\delta k_d(\dot{u}_d-\hat{z}_2)-r\delta_z^2+\delta_z k_f\hat{M}_c\\&\quad+k_p^{T}\vartheta^{-1}\dot{k}_p+k_d^{T}\zeta^{-1}\dot{k}_d+M_c^{T}\varepsilon^{-1}\dot{M}_c\end{aligned} \tag{43}$$

Substituting formula (24) into the above formula can obtain

$$\begin{aligned}\dot{V}&=s(w_1\dot{e}_1+z_3+\dot{u}_d-w_1\dot{e}_1-z_3-w_2s-\dot{u}_d)-a\delta^2+\delta k_p(U_s-\hat{z}_1)+\delta k_d(\dot{u}_d-\hat{z}_2)\\&\quad-r\delta_z^2+\delta_z k_f\hat{M}_c+k_p^{T}\vartheta^{-1}\dot{k}_p+k_d^{T}\zeta^{-1}\dot{k}_d+M_c^{T}\varepsilon^{-1}\dot{M}_c\\&=-w_2s^2-a\delta^2+\delta k_p(U_s-\hat{z}_1)+\delta k_d(\dot{u}_d-\hat{z}_2)-r\delta_z^2+\delta_z k_f\hat{M}_c+k_p^{T}\vartheta^{-1}\dot{k}_p\\&\quad+k_d^{T}\zeta^{-1}\dot{k}_d+M_c^{T}\varepsilon^{-1}\dot{M}_c\\&\le-w_2s^2-a\delta^2+\delta k_p(U_s-\hat{z}_1)+\delta k_d(\dot{u}_d-\hat{z}_2)-r\delta_z^2+\delta_z k_f\hat{M}_c-k_p^{T}\vartheta^{-1}\dot{k}_p\\&\quad-k_d^{T}\zeta^{-1}\dot{k}_d-M_c^{T}\varepsilon^{-1}\dot{M}_c\end{aligned} \tag{44}$$

Substituting formulas (36), (37) and (38) into the above formula can obtain

$$\begin{aligned}\dot{V}&\le-w_2s^2-a\delta^2+\delta k_p(U_s-\hat{z}_1)+\delta k_d(\dot{u}_d-\hat{z}_1)-r\delta_z^2+\delta_z k_f\hat{M}_c\\&\quad-k_p^{T}\vartheta^{-1}[\delta k_p(U_s-\hat{z}_1)\vartheta]/k_p-k_d^{T}\zeta^{-1}[\delta k_d(\dot{u}_d-\hat{z}_2)\zeta]/k_d\\&\quad-M_c^{T}\varepsilon^{-1}\varepsilon\delta_z k_f\dot{z}\end{aligned} \tag{45}$$

Simplification of the above formula can obtain

$$\dot{V} \leq -w_2 s^2 - a\delta^2 - r\delta_z^2 \tag{46}$$

where $w_2$, $a$ and $r$ are positive parameters, the above formula can be written as

$$\dot{V} \leq 0 \tag{47}$$

It can be obtained that the Lyapunov function (41) is bounded.

According to Barbalat theorem, we can get

$$\lim_{t\to\infty} s(t) = 0, \quad \lim_{t\to\infty} \delta(t) = 0, \quad \lim_{t\to\infty} \delta_z(t) = 0 \tag{48}$$

By Lyapunov theory, $\hat{k}_p$, $\hat{k}_d$ and $\hat{M}_c$ are bounded, tracking error is also bounded and converges to zero neighborhood, all signals of the system are bounded.

**5. Simulation Results and Discussions**

In this part, MATLAB is used for simulation test. The initial value of attitude angles are [0,0,0] rad, and the initial value of altitude is 0 m. The parameters of the quadrotor and the controller are given in the Table 1 and Table 2 respectively.

Table 1: Parameters of the quadrotor model

| Symbol | Description | Value |
|---|---|---|
| $k_f$ | Coefficient of air resistance | $0.15\ Ns^2 / rad^2$ |
| $m$ | Mass of the quadrotor | $10\ kg$ |
| $g$ | Gravitational acceleration | $9.8\ m/s^2$ |
| $I_x$ | Inertial moment along x-axis | $1\ kg \cdot m^2$ |
| $I_y$ | Inertial moment along y-axis | $1\ kg \cdot m^2$ |
| $I_z$ | Inertial moment along z-axis | $2\ kg \cdot m^2$ |
| $l$ | length of the quadrotor arm | $0.3\ m$ |

Table 2: Parameters of the controller

| | $w_1$ | $w_2$ | $k_p$ | $k_d$ | $\omega$ | $b_0$ |
|---|---|---|---|---|---|---|
| $Z$ | 70 | 5 | 600 | 7 | 50 | 1 |
| $\phi$ | 72 | 40 | 650 | 15 | 50 | 1 |
| $\theta$ | 80 | 40 | 620 | 18 | 50 | 1 |
| $\psi$ | 70 | 50 | 890 | 36 | 50 | 1 |

**Example 1**: In this test, the mass of the load is kept unchanged, and m=5 kg. The input signals of the system are $Z_d = 5$, $\phi_d = 30^o$, $\theta_d = 45^o$, $\psi_d = 60^o$, and the simulation results are compared with those of LADRC. Fig.4 and Fig.5 show the output curves and the error curves of the system. This result show that the response speed of the designed scheme is obviously faster than that of LADRC. In the pitch angle channel and roll angle channel, the overshoot of SMC-LADRC is smaller than that of LADRC, and the designed scheme realizes the tracking of the input signal in 0.5 seconds, while the LADRC realizes the stable tracking in 1.5 seconds, which indicates that the designed control scheme is obviously better than LADRC, and it has fast response speed and stable tracking performance, thus proving that the SMC-LADRC scheme designed in the paper is effective.

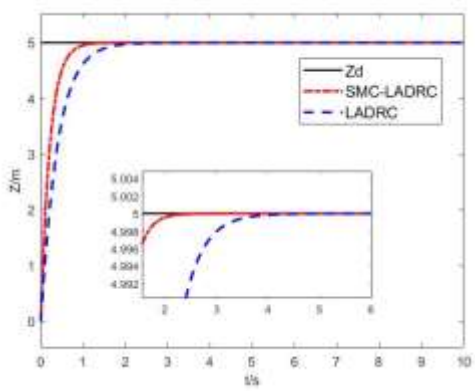


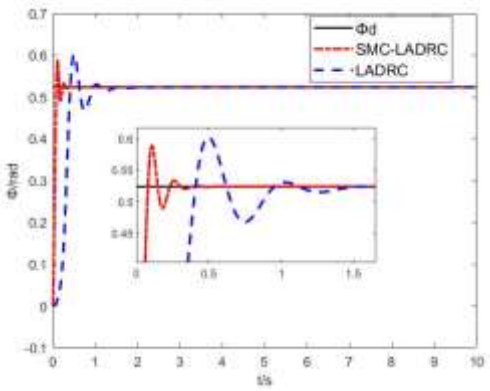

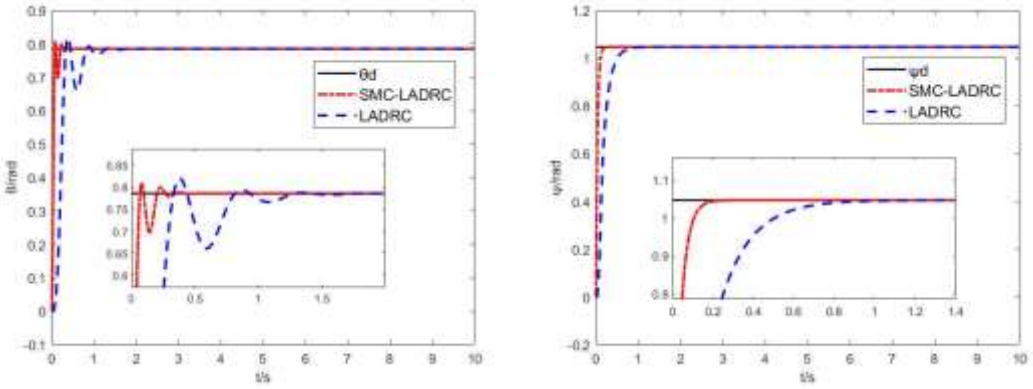


Fig.4 The tracking output curves

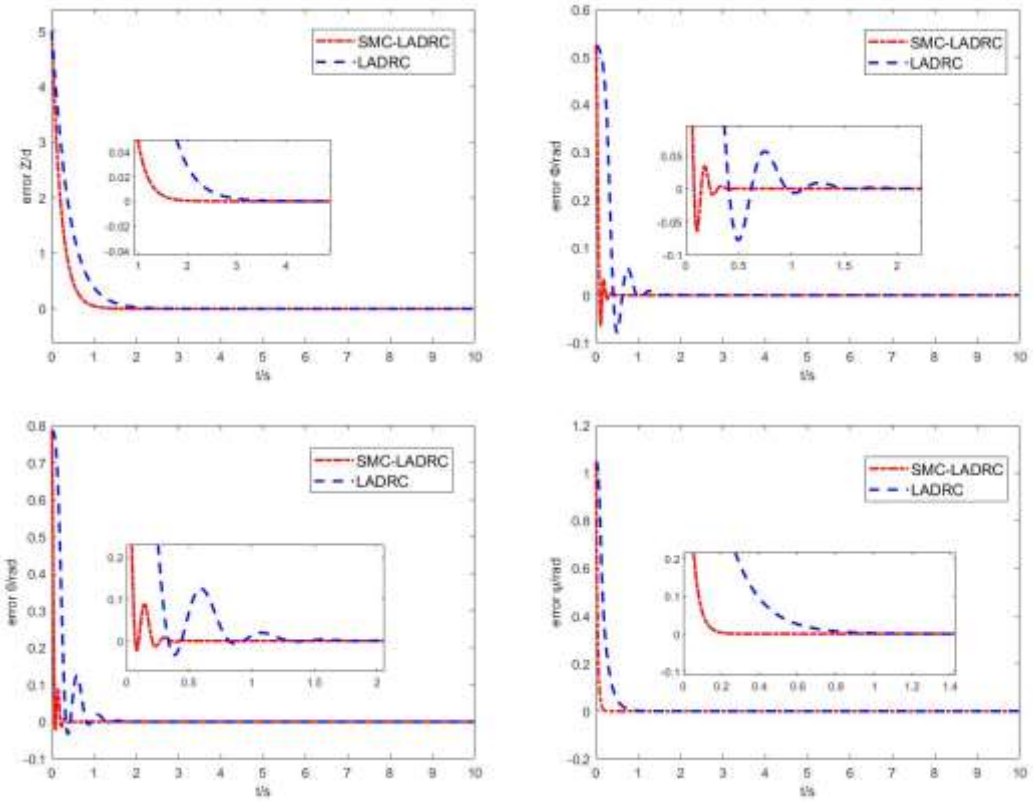


Fig.5 The error curves

**Example 2**: In this test, in order to test the control performance of the designed method and LADRC under the same bandwidth, keeping the parameters and input signals unchanged. Gaussian noise with mean value of 0 and variance of 2 is introduced to simulate the noise disturbance in the process of quadrotor flight. Fig.6 is simulation diagram of Gaussian noise. Fig.7 shows the adaptive curves of $k_p$ and $k_d$. The

output curves and error curves under Gaussian noise are given in Fig.8 and Fig.9.

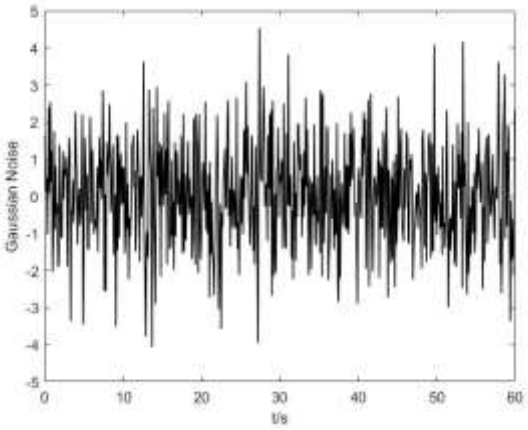


Fig.6 Gaussian noise simulation diagram

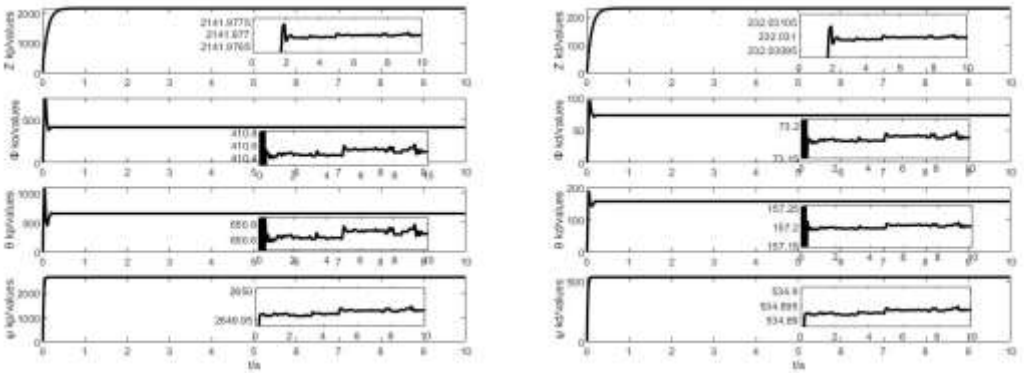

Fig.7 Adaptive adjustment curves for $k_p$ and $k_d$

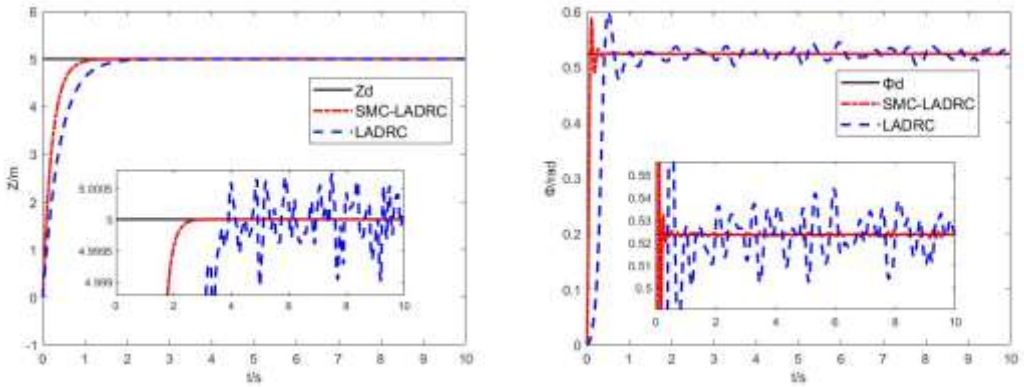

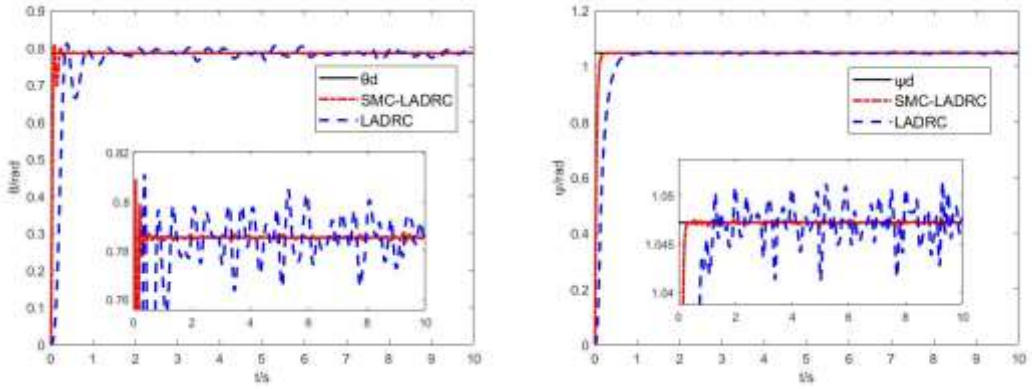


Fig.8 The output curves under Gaussian noise

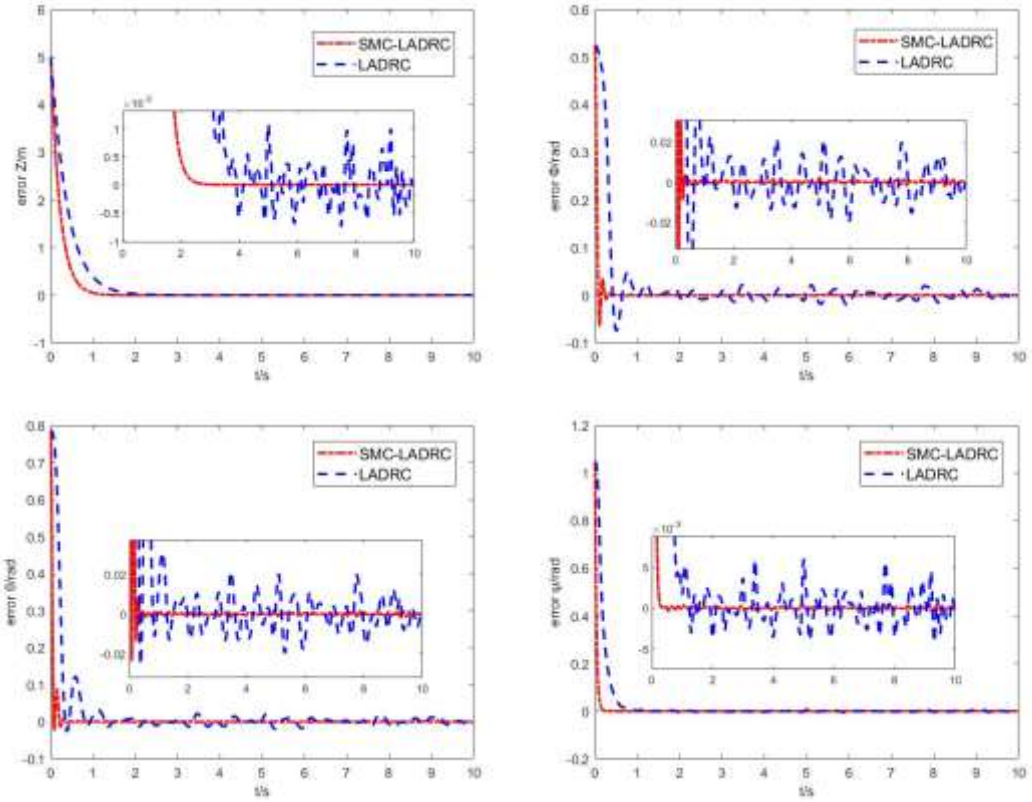


Fig.9 The error curves under Gaussian noise

Through the analysis of Fig.7, it can be clearly seen that the values of $k_p$ and $k_d$ are adjusted in real time, indicating that the introduction of adaptive law is effective, which can adjust the parameters in real time according to the state of the system. In addition, it can eliminate the parameter deviation and improve the control precision. Fig.8 and Fig.9 clearly show that when the bandwidth is the same, the tracking curves of SMC-

LADRC has smaller fluctuation, while the fluctuation of LADRC is larger. This indicates that the introduction of robust SMC is effective, it can well overcome the problem of low control precision caused by the limited bandwidth of LADRC, which improve the anti-disturbance performance of the system.

**Example 3**: The load mass of the quadrotor load UAV in practical application may be constantly changing. In this test, keeping the input and parameters of the system unchanged, and use the mass variation as an disturbance, the simulation results are compared with those of SMC-LADRC without the adaptive of mass. Fig.10 shows the variation of load mass $m$. The output curves of the system with the mass variation is given in Fig.11. Fig.12 shows the error curves.

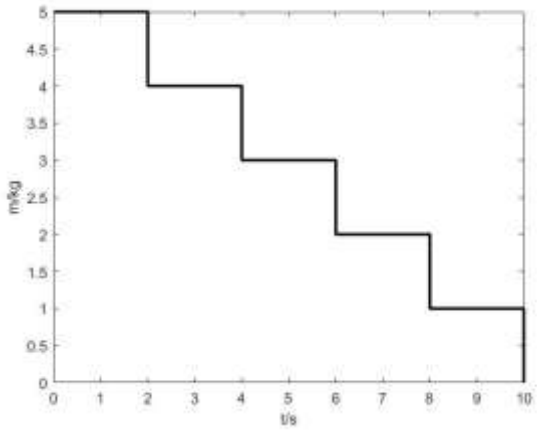


Fig.10 Load mass variation diagram

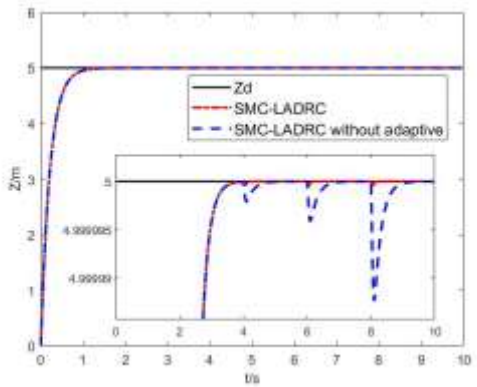


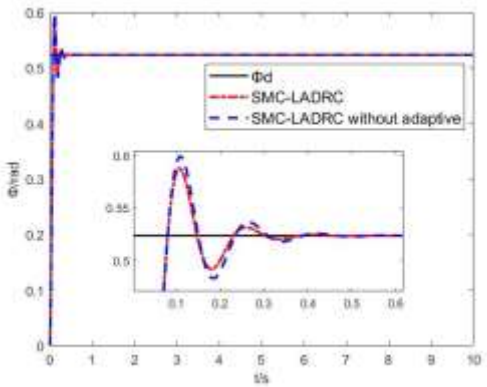

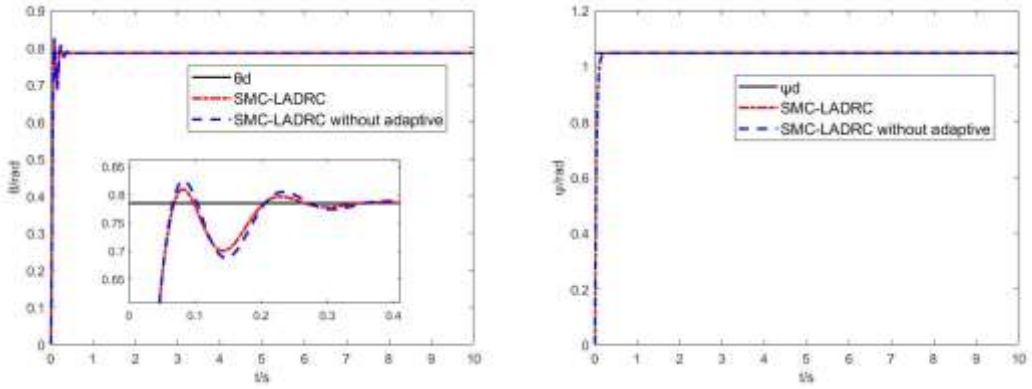


Fig.11 The output curves with mass variation

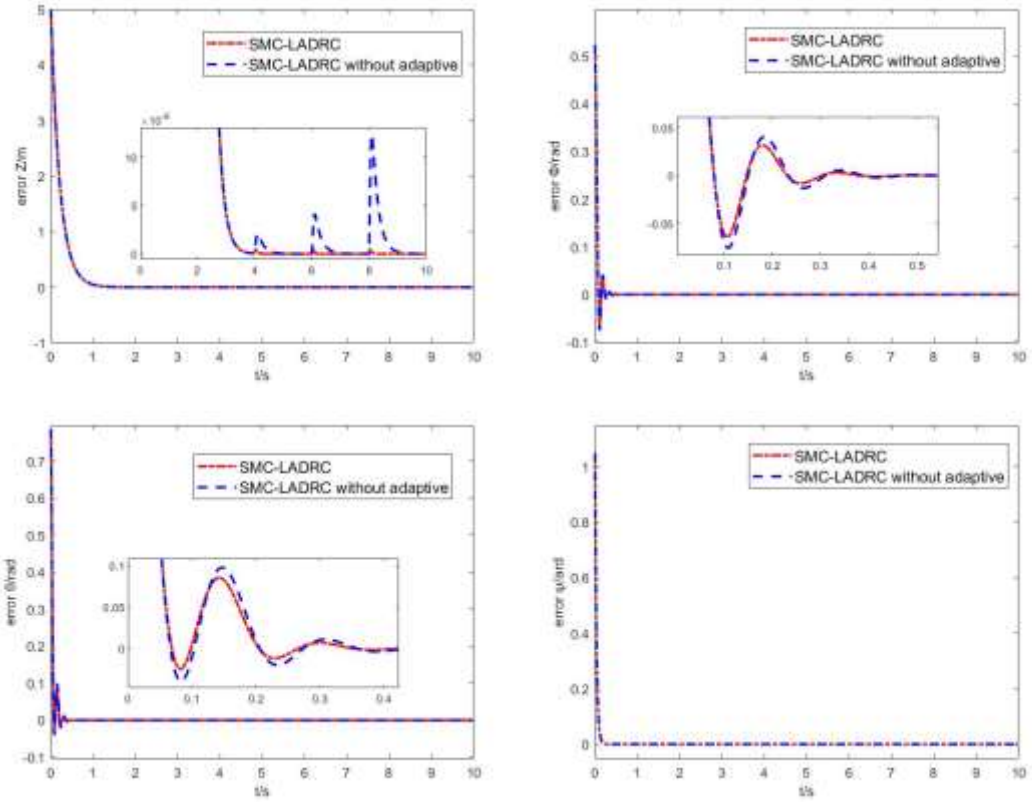


Fig.12 The error curves with mass variation

Through the analysis of Fig.11 and Fig.12, it can be seen that the SMC-LADRC with mass adaptive law can well reduce the influence of mass variation on the altitude channel. In the pitch angle and roll angle channels, the overshoot of the proposed scheme is smaller than that of the one without mass adaptive. However, in the yaw angle channel, the difference between the output curves and the error curves of the two

is very small, which can be seen from the quadrotor mathematical model in formula (13) that the mass variation has no direct effect on the yaw channel. Through the analysis of the simulation results, it can be obtained that the designed mass adaptive law is effective, which can reduce the influence of mass variation on the quadrotor.

## 6. Conclusion

In this paper, considering the mass variation of the quadrotor in practical application, the dynamic model of a quadrotor load UAV is established, and a composite control scheme combining robust SMC and LADRC is proposed. The LADRC is used to estimate and compensate the disturbances, but it is limited by the bandwidth, which leads to the decrease of its control precision. The introduction of SMC can further improve the robustness of the system and overcome the problem of low control precision caused by limited bandwidth. In addition, introducing adaptive law to adjust the adjustable parameters in real time is to simplify the parameter setting process of the controller, which is beneficial to the stability analysis of the whole system. Moreover, considering the mass variation of the quadrotor, an adaptive law is designed for real-time control. The Lyapunov stability theory proves that the system is stable. Finally, the simulation results are compared with LADRC to verify the superiority and effectiveness of the designed scheme, and the proposed mass adaptive law is also effective. In the future work, we will study the feasibility of the designed method in the practical application and improve it according to experiments.

## Declarations

**Funding:** No funding was received to assist with the preparation of this manuscript.

**Conflicts of interest/Competing interests:** The authors declare that they have no conflict of interest.

**Availability of data and material：** All data generated or analyzed during this study are included in this article.

**Authors' contributions:** The first draft of the manuscript was written by Zhaoji Wang and all authors commented on previous versions of the manuscript. All authors read and approved the final manuscript.

**Consent for publication:** This article has not been published previously, it is not under consideration for publication elsewhere.

**References**


1. Zhang, J., Ren, Z., Deng, C., Wen, B.: Adaptive fuzzy global sliding mode control for trajectory tracking of quadrotor UAVs. Nonlinear Dynamics. **97**(1), 609-627 (2019)
2. Zou， Y., Zhu, B.: Adaptive trajectory tracking controller for quadrotor systems subject to parametric uncertainties. Journal of the Franklin Institute. **354** (15), 6724-6746 (2017)
3. Ramirez-Rodriguez, H., Parra-Vega, V., Sanchez-Orta, A., Garcia-Salazar, O.: Robust backstepping control based on integral sliding modes for tracking of quadrotors. Journal of Intelligent & Robotic Systems. **73**, 51–66 (2014)
4. Mc, A., Lta, B.: Robust PID control of quadrotors with power reduction analysis. ISA Transactions. **98**, 47-62 (2020)
5. Najm, A., Ibraheem, I.: Nonlinear PID Controller Design for a 6-DOF UAV Quadrotor System. Engineering Science & Technology an International Journal. **22** (4), 1087-1097 (2019)
6. Outeiro, P., Cardeira, C., Oliveira, P.: Multiple-model adaptive control architecture for a quadrotor with constant unknown mass and inertia. Aerospace Science and Technology. **117**, 106899 (2021)
7. Chen, L., Liu, Z., Gao, H., Wang, G.: Robust adaptive recursive sliding mode attitude control for a quadrotor with unknown disturbances. ISA Transactions. (2021).

8. Hamid, G., Maedeh, E., Hamed, K.: Adaptive super-twisting non-singular ter minal sliding mode control for tracking of quadrotor with bounded disturbanc es. Aerospace Science and Technology. **112**(1), 106616 (2021)
9. Labbadi, M., Boukal, Y., Cherkaoui, M., Djemal, M.: Fractional-order global sliding mode controller for an uncertain quadrotor UAVs subjected to external disturbances. Journal of the Franklin Institute. **358**(9), 4822-4847 (2021)
10. Zhang, Z., Chen, T., Zheng, L.: A multilayer neural dynamic controller design method of quadrotor UAV for completing time-varying tasks. Nonlinear Dynamics. **104**(4), 3597-3616 (2021)
11. Han, J.: From PID to Active Disturbance Rejection Control. IEEE Transactions on Industrial Electronics. **56** (3), 900-906 (2009)
12. Chang, K., Xia, Y., Huang, K., Ma, D.: Obstacle avoidance and active disturbance rejection control for a quadrotor. Neurocomputing. **19**, 60-69 (2016)
13. Bouzid, Y., Siguerdidjane, H., Guiatni, M., Lamraoui, HC.: Reinforcement of a Reference Model-based Control using Active Disturbance Rejection principle: application to quadrotor. IFAC-PapersOnLine. **52**(12), 152-157 (2019)
14. Wei, D., Gu, G., Zhu, X., Ding, H.: A high-performance flight control approach for quadrotors using a modified active disturbance rejection technique. Robotics and Autonomous Systems. **83**, 177-187 (2016)
15. Luo, S., Sun, Q., Sun, M., Tan, P., Wu, W., Sun, H., Chen, Z.: On decoupling trajectory tracking control of unmanned powered parafoil using ADRC-based coupling analysis and dynamic feedforward compensation. Nonlinear Dynamics.

**92**(4), 1619-1635 (2018)

16. Zhu, E., Pang, J., Sun, N., Gao, H., Sun, Q., Chen, Z.: Airship horizontal trajectory tracking control based on Active Disturbance Rejection Control. Nonlinear Dynamics. **75**(4), 725-734 (2014)
17. Gao, Z.: Scaling and bandwidth-parameterization based controller tuning. Proceedings of the 2003 American Control Conference, Denver, CO, USA, pp. 4989-4996 (2003)
18. Zhang, Y., Chen Z., Zhang, X., Sun, Q., Sun, M.: A novel control scheme for quadrotor UAV based upon active disturbance rejection control. Aerospace Science and Technology. **79**, 601-609 (2018)
19. Guo, B., Bacha, S., Alamir, M., Mohamed, A., Boudinet, C.: LADRC applied to variable speed micro-hydro plants: Experimental validation. Control Engineering Practice. **85**, 290-298 (2019)
20. Wang, Y., Tan, W., Cui, W., Han, W., Guo, Q.: Linear active disturbance rejection control for oscillatory systems with large time-delays. Journal of the Franklin Institute. (2021)
21. Hou, G., Gong, L., Wang, M., Yu, X., Yang, Z., Mou, X.: A novel linear active disturbance rejection controller for main steam temperature control based on the simultaneous heat transfer search. ISA Transactions. (2021)
22. Wu, J., Peng, H., Chen, Q., Peng, X.: Modeling and control approach to a distinctive quadrotor helicopter. ISA Transaction. **53**(1), 173-185 (2014)
23. Cai, Z., Lou, J., Zhao, J., Wu, K., Liu, N., Wang, Y.: Quadrotor trajectory tracking

and obstacle avoidance by chaotic grey wolf optimization-based active disturbance rejection control. Mechanical Systems and Signal Processing. **128**, 636-654 (2019)

24. Zhao, Z., Cao, D., Yang, J., Wang, H.: High-order sliding mode observer-based trajectory tracking control for a quadrotor UAV with uncertain dynamics. Nonlinear Dynamics. **102**(4), 2583-2596 (2020)
25. Eskandarpour, A., Sharf, I.: A constrained error-based MPC for path following of quadrotor with stability analysis. Nonlinear Dynamics. **99**(2), 899-918 (2020)
26. Tang, P., Lin, D., Zheng, D., Fan, S., Ye, J.: Observer based finite-time fault tolerant quadrotor attitude control with actuator faults. Aerospace Science and Technology. **104**, 105968 (2020)
27. Hua, C., Wang, K., Chen, J., You, X.: Tracking differentiator and extended state observer-based nonsingular fast terminal sliding mode attitude control for a quadrotor. Nonlinear Dynamics. **94**(1), 343-354 (2018)
28. Wang, B., Yu, X., Mu, L., Zhang, Y.: Disturbance observer-based adaptive fault-tolerant control for a quadrotor helicopter subject to parametric uncertainties and external disturbances. Mechanical Systems and Signal Processing. **120**, 727-743 (2019)
29. Liu, W., Zhao, T.: An active disturbance rejection control for hysteresis compensation based on Neural Networks adaptive control. ISA Transactions. **109**, 81-88 (2021)
30. Nguyen, S., Lam, B., Ngo, V.: Fractional-order sliding-mode controller for semi-active vehicle MRD suspensions. Nonlinear Dynamics. **101**(2), 795-821 (2020)

31. Hovakimyan, N., Nardi, F., Calise, A., Kim, N.: Adaptive output feedback control of uncertain nonlinear systems using single-hidden-layer neural networks. IEEE Transactions on Neural Networks. **13**(6), 1420-1431 (2002)

32. Zhao, T., Tan, Y.: Adaptive H∞ RBFN tracking control for nonlinear systems with unknown hysteresis. In: IEEE International Symposium on Intelligent Control, Taipei, Taiwan, 2-4 September, pp.352-356. (2004) IEEE.